NEUROSCIENCE

Adult neural stem cells have latent inflammatory potential that is kept suppressed by *Tcf4* to facilitate adult neurogenesis

Mohammad Shariq[1,2], Vinaya Sahasrabuddhe[1], Sreevatsan Krishna[1], Swathi Radha[1], Nruthyathi[1], Ravishankara Bellampalli[1], Anukriti Dwivedi[1], Rajit Cheramangalam[1], Boris Reizis[3], Jean Hébert[4], Hiyaa S. Ghosh[1]*

Inflammation is known to adversely affect adult neurogenesis, wherein the source of inflammation is largely thought to be extraneous to the neurogenic niche. Here, we demonstrate that the adult hippocampal neural progenitors harbor an inflammatory potential that is proactively suppressed by transcription factor 4 (*Tcf4*). Deletion of *Tcf4* in hippocampal *nestin*-expressing progenitors causes loss of proliferative capacity and acquisition of myeloid inflammatory properties. This transformation abolishes their differentiation potential and causes production of detrimental factors that adversely affect niche cells, causing inflammation in the dentate gyrus. Thus, on one hand, *Tcf4* deletion causes abrogation of proliferative progenitors leading to reduction of adult neurogenesis, while on the other, their accompanying inflammatory transformation inflicts inflammation in the niche. Taken together, we provide the first evidence for a latent inflammatory potential of adult hippocampal neural progenitors and identify *Tcf4* as a critical regulator that facilitates adult neurogenesis via proactive suppression of this detrimental potential.

INTRODUCTION

Adult neurogenesis, the process by which new neurons in the adult brain are continually generated in specific locations, is known to be environmentally responsive. While enriched environment enhances adult neurogenesis (*1*–*3*), stress (*4*–*6*), aging, and inflammation (*7*–*9*) adversely affect adult neurogenesis. Studies have established that in the mammalian brain, inflammation such as that caused by bacterial mimetics or accumulated during aging reduces adult neurogenesis, in turn affecting cognition. Parabiosis experiments have further shown that inflammatory factors from aging circulation can affect adult neurogenesis (*10*, *11*), thereby suggesting a central nervous system (CNS) extraneous inflammation influence on this process. In a similar vein, neural precursor cell proliferation in the neurogenic niche has been shown to be regulated by the peripheral immune system, without requiring the direct presence of immune cells in the brain parenchyma (*12*–*15*). While these studies establish a cross-talk between immune signaling and the adult neurogenic niche, a potential cell-intrinsic role of the adult neural progenitors in inflammatory response and/or related processes in the CNS remain unexplored.

A recent transcriptomic study of ex vivo adult neural precursor culture revealed an enriched immune gene signature specific to the proliferative subset of these precursor cells (*16*); however, the potential physiological relevance of this gene ontology remains unclear. In the context of immune gene signature, another study in the subventricular zone (SVZ) neurogenic niche has revealed that a subset of adult neural stem cells (aNSCs) in the aged brain up-regulates interferon (IFN) signaling in response to T cell infiltration (*17*). This suggested that under certain circumstances, the aNSC could up-regulate an inflammatory response. However, whether the adult NSC indeed harbors an innate inflammatory potential under homeostatic conditions and, if so, what are the regulators that manage this detrimental potential remain unexplored.

The basic helix-loop-helix transcription factor 4 (*Tcf4*), a gene implicated in schizophrenia (SCZ) (*18*) and Pitt-Hopkins syndrome (PTHS) (*19*–*21*), is widely and continually expressed in the adult brain parenchyma (*22*–*24*). *Tcf4* belongs to the E-protein transcription factor family, which has been broadly implicated in cell fate decisions in the immune system (*25*). Specifically, *Tcf4* has been shown to be critically required for both differentiation and cell fate maintenance of a lympho-myeloid immune cell type, the plasmacytoid dendritic cells (*26*, *27*). In the context of neural stem cells, overexpression of E-protein constructs was used to show its role in NSC differentiation in the SVZ (*28*). Other studies have implicated *Tcf4* in differentiation, maturation, and migration of neurons during brain development (*29*–*32*). While the above studies demonstrate the importance of *Tcf4* during embryonic brain development, its role in adult neural stem cells remains to be elucidated.

It is important to note that the context and process of adult neurogenesis are different from embryonic neurogenesis in many ways; for instance, adult neurogenesis is specifically responsive to environmental and systemic cues. Therefore, it is conceivable that the full spectrum of fate potential of the adult NSC would be more diverse than the embryonic NSC that reside in a rather contained environment. Here, we reveal a previously unknown aspect of the adult hippocampal neural progenitors: that they harbor a latent myeloid inflammatory potential, which needs to be proactively suppressed for maintaining their proliferative and differentiation capacity. Furthermore, we identify *Tcf4* as a critical regulator that keeps the inflammatory potential of aNSCs suppressed to facilitate normal adult neurogenesis.

RESULTS

Tcf4 is expressed in cells of the hippocampal adult neurogenic program

We observed that *Tcf4* is highly expressed in the adult brain neurogenic niches, both in the subgranular zone (SGZ) of the hippocampus

[1]National Centre for Biological Science, Tata Institute of Fundamental Research (NCBS-TIFR), Bangalore, India. [2]The University of Trans-Disciplinary Health Sciences and Technology, Bangalore, India. [3]Department of Pathology, New York University Grossman School of Medicine, New York, NY, USA. [4]Departments of Neuroscience and Genetics, Albert Einstein College of Medicine, New York, NY, USA.
*Corresponding author. Email: hiyaa@ncbs.res.in

(Fig. 1A) and the SVZ of the lateral ventricles (fig. S1A), as marked by *nestin-GFP* colocalization. Because *Tcf4* is known to be expressed in mature granule neurons of the *dentate gyrus* (DG) (*22*), we used the *nestin*CreERt2-*Stop*-EGFP genetic reporter to identify the sparse population of hippocampal neural stem cells and their progeny in the DG and investigated Tcf4 protein expression at different stages of the entire hippocampal adult neurogenic program. For this, we initiated Cre-induced enhanced green fluorescent protein (EGFP) expression in the *nestin*-expressing aNSC and identified GFP-expressing neural stem cells and their immediate progeny 3 weeks after GFP induction. The different cell stages during the hippocampal adult neurogenic program were identified on the basis of the well-established cell markers and cell morphology as described in Fig. 1B and shown in Fig. 1C. We then quantified Tcf4 protein expression in these different cell stages, starting from the radial glia-like (RGL) cells to intermediate proliferating cells (IPCs), neuroblast, and immature neurons, relative to the Tcf4 expression in mature granule cell (GC) in the DG. This showed that Tcf4 is expressed throughout the hippocampal neurogenic program, with peak expression at the immature neuron stage (Fig. 1D).

Tcf4 expression in NSC is required for hippocampal adult neurogenesis

Given the high expression of Tcf4 in the adult neurogenic niche, we investigated the role of *Tcf4* in the aNSC through inducible deletion of *Tcf4* in *nestin*-expressing stem/progenitor cells in the adult brain using the *nestin*CreERt2; Tcf4-*flox* [knockout (KO)] transgenic line. First, we confirmed deletion in our KO animals by detecting LoxP recombination by genotyping polymerase chain reaction of microdissected DG in the wild-type (WT; *nestin*CreERt2; *Tcf4-wt*) and KO animals, as shown in fig. S2A. Next, we examined the effect of *Tcf4* deletion in aNSC on adult neurogenesis by investigating the newborn neurons in the DG. We observed that *Tcf4* deletion in aNSC resulted in a significant reduction in the number of double-cortin$^+$ (DCX) newborn neurons in KO DG when compared to the WT (Fig. 2, A and B, and fig. S2B), indicating impaired adult hippocampal neurogenesis.

To examine whether *Tcf4* deletion affects the proliferation and differentiation of aNSC, we performed a 5-bromo-2′-deoxyuridine (BrdU) pulse-chase experiment (Fig. 2C). For this, BrdU pulse was given for 7 days to WT and KO animals, followed by 14 days of chase to assess whether proliferating cells become newborn neuron after *Tcf4* deletion. Assessment of BrdU$^+$ cells at the end of the chase period showed a significant reduction in proliferation in the KO DG as shown by fewer BrdU$^+$ cells (Fig. 2, D and E, and fig. S2C). Furthermore, the number of BrdU$^+$ cells adopting a neuronal fate, as marked by coexpression of DCX and BrdU, were also reduced (Fig. 1, D and F, and fig. S2D). Consistently, the number of Tbr2 expressing IPC in the SGZ was significantly reduced in the KO DG (Fig. 2, G and H, and fig. S2E). Also, when progenitors from the adult WT and KO animals were cultured in vitro, we observed a marked reduction in the neurosphere counts from KO brains (fig. S2, F and G), indicating a deficit in the proliferating progenitor population.

Tcf4 expression in hippocampal adult NSC is required for neuronal fate acquisition

To track the fate of the *nestin*-expressing progenitors after *Tcf4* deletion in vivo, we performed genetic reporter–based lineage tracing (Fig. 3A) using the *nestin*CreERt2; Tcf4*wt* or *flox*; *Rosa-flox*-Stop-*flox*-EGFP mice. In this, tamoxifen-induced *Cre* activation results in indelible marking of the *nestin*CreER-expressing cells, along with *Tcf4* deletion in the Tcf4-*flox* mice (KO), while in *Tcf4-wt* mice (WT) that do not have loxP-flanking locus, the GFP-expressing cells remain *Tcf4*-undeleted. Colocalization of *nestin*-GFP with DCX, to identify immature neurons at day 30 (Fig. 3B), and with Calbindin or PROX1 (Prospero Homeobox 1) for mature granule neurons at day 60

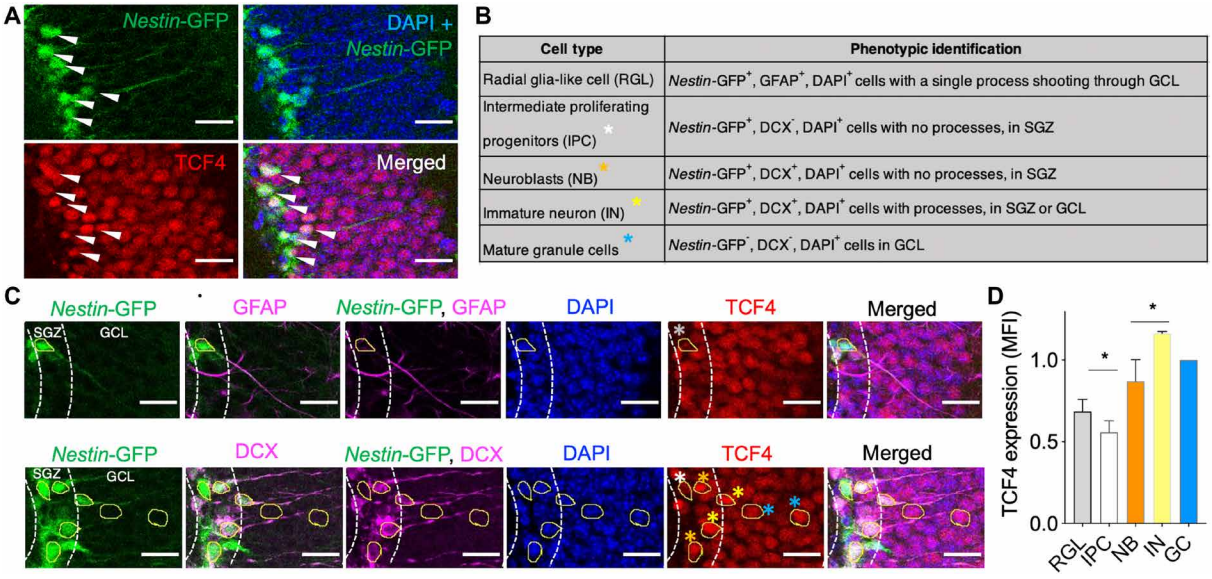

Fig. 1. Tcf4 is expressed in hippocampal adult neurogenic cells. (**A**) Tcf4 protein expression in the SGZ in adult brain DG. DAPI, 4′,6-diamidino-2-phenylindole. (**B**) Description for cell type identification used in (C) based on stage-specific marker colocalization and morphology [colored asterisks depict distinct cell types shown on the TCF4 image in (C)]. GCL, Granule Cell Layer. (**C**) Representative immunofluorescence images showing Tcf4 expression in cells at various stages of adult hippocampal neurogenesis, showing RGL in the top and the other cell types in the bottom; dotted curved lines mark the SGZ area. (**D**) Tcf4 protein quantitation in different cell stages from (B) and (C) normalized to mature granule cells. Quantitation from three brains; error bar represents SD (unpaired *t* test; $^*P < 0.03$). Scale bars, 25 μm. MFI, mean fluorescence intensity.

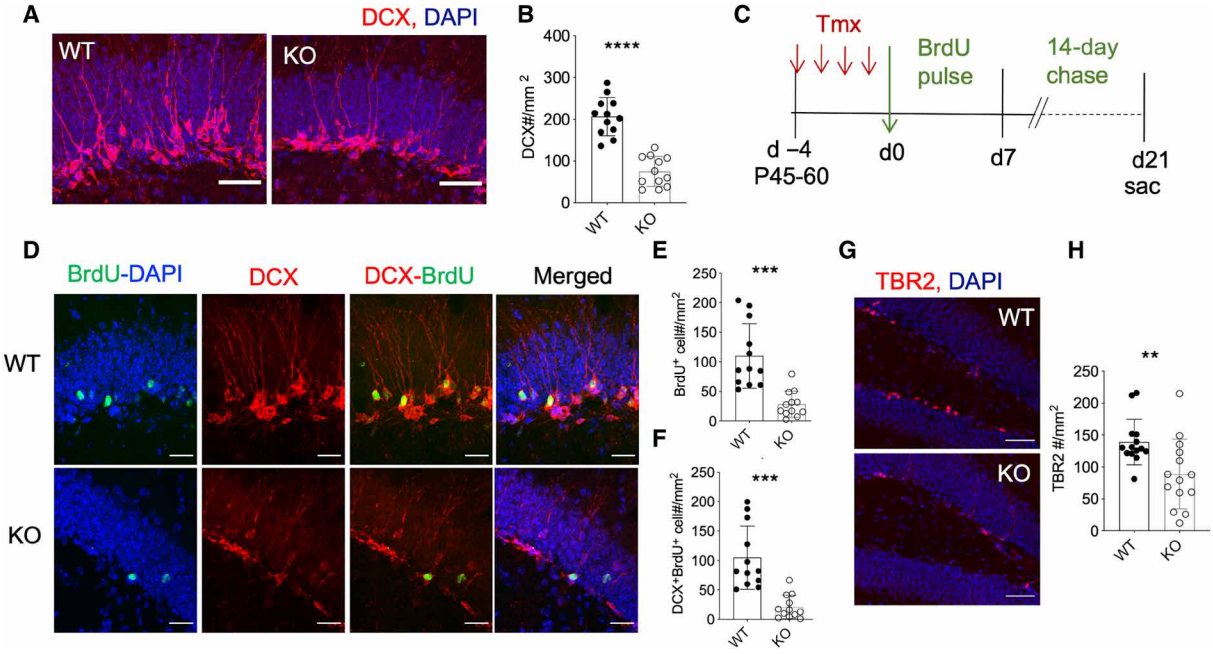

Fig. 2. Tcf4 is required for hippocampal adult neurogenesis. (**A**) Representative image of DCX$^+$ immature neuron in the WT or KO adult brain DG. (**B**) Quantitation from (A). (**C**) Schematic for BrdU pulse-chase experiment. (**D**) Representative image from BrdU pulse-chase experiment. Scale bars, 25 μm. (**E** and **F**) Quantitation of cells after 14 days of chase from (D). (**G** and **H**) Representative images (G) and quantification (H) of Tbr2+ve IPC in DG 30 days after deletion. Scale bars, 50 μm. Counts are from three to five brains, each dot represents a section from a brain, and error bar represents SD (unpaired *t* test; $^{**}P < 0.003$, $^{***}P < 0.0003$, and $^{****}P < 0.0001$).

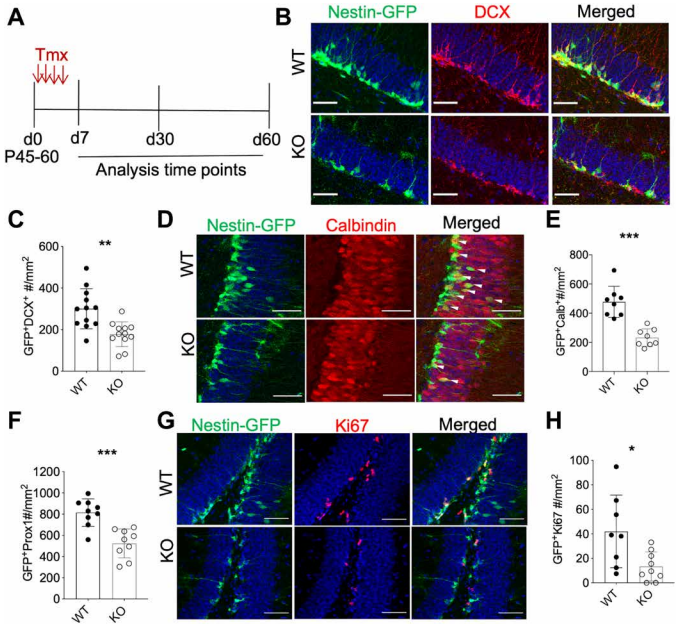

Fig. 3. Genetic lineage tracing shows fewer adult born neurons from *Tcf4*-deleted *nestin*-expressing progenitors. (**A**) Schematic for genetic lineage tracing experimental regime. (**B** and **C**) Representative images (B) quantitation (C) of genetic reporter-based tracing of progenitors 30 days after deletion for DCX expression. (**D**) Genetic reporter-based tracing of progenitors 60 days after deletion for Calbindin expression. (**E** and **F**) Quantitation of genetically traced Calbindin+ve and Prox1+ve mature neurons. (**G** and **H**) Representative images (G) quantitation (H) of genetic lineage tracing for Ki67+ve progeny at day 7 after deletion. $n = 3$ animals per genotype, each dot represents a section from a brain, and error bar represents SD. (unpaired *t* test, $^{*}P < 0.01$, $^{**}P < 0.001$, and $^{***}P < 0.0003$). Scale bars, 50 μm.

after deletion (Fig. 3D and fig. S3A) was used to assess neuronal fate acquisition for GFP lineage traced progeny. Quantification of the genetically traced progeny confirmed that fewer progenitors attained the neuronal fate in KO brains, as indicated by reduced GFP$^+$ DCX$^+$ (Fig. 3C and fig. S3B), GFP$^+$ Calbindin$^+$ (Fig. 3E and fig. S3C), and GFP$^+$ PROX1$^+$ cells (Fig. 3F and fig. S3D). Furthermore, consistent with a reduction in progenitors, the KO brains showed reduced numbers of GFP$^+$ Ki67$^+$ progeny (Fig. 3, G and H, and fig. S3E). To further examine the early proliferating cell populations after *Tcf4* deletion in *nestin*-expressing progenitors, we performed another lineage tracing experiment but, this time, along with a BrdU pulse-chase regime, as described in fig. S3F. The 5 days BrdU pulse immediately after deletion allowed us to examine the proliferating population at an acute stage (within 6 days) of proliferation, while the GFP$^+$ lineage tracing allowed us to examine cell fate at 11 days after deletion. We performed absolute counts for proliferating cells throughout the DG, which showed that the proliferating cell population (fig. S3G) was markedly decreased within the first few days after *Tcf4* deletion. This included the Sox2$^+$ and the Tbr2$^+$ progenitors (fig. S3, H and I). Furthermore, analysis of neuroblasts also showed marked reduction (fig. S3, J and K). We also traced the GFP+ve cells to assess their developmental stage at 11 days after deletion. This further showed a marked reduction in early progenitors (fig. S3M), neuroblast (fig. S3, N and O), immature neuron (fig. S3P), and granule neuron (fig. S3Q). These results further confirmed that the impact of *Tcf4* deletion in aNSC is at the level of proliferating progenitor cell stage. However, these observations do not preclude a possible important role in later stages for *Tcf4*, for which investigations with a later cell stage–specific deletion, such as using DCX-CreER will provide further insight.

Astrocytes are known to express low levels of Nestin; therefore, to ensure that *nestin*-mediated CreER is not influencing the astrocytic

population in the DG niche, we investigated astrocytes through S100-beta labeling for possible *nestin*-CreER–induced GFP expression. As shown in fig. S3R, none of the astrocytes showed GFP expression, confirming that there was no Cre expression in niche astrocytes, thereby ruling out any nonspecific effects. Furthermore, the GFP tracing also confirmed that *Tcf4* deletion in aNSC does not lead to fate diversion to the astrocytic lineage.

Reduced adult neurogenesis is known to affect hippocampus-based cognition such as contextual and spatial memory (*33*, *34*). Therefore, we also validated the impact of *Tcf4* deletion–mediated reduction of adult neurogenesis at the behavior level. For this, we performed "novel location recognition (NLR)" test, a hippocampal adult neurogenesis–dependent (*35*) memory task. As shown in Fig. 4A, the KO mice did not show a preference for the newly located object, indicating poor spatial memory acquisition during training leading to poor performance during test. As shown in Fig. 4 (B and C), the exploration of either location during training and the total time of exploration during test did not vary between WT and KO mice.

Tcf4 deletion in neural progenitors results in their transformation into a myeloid-like inflammatory cell state

Our observations indicated that *Tcf4* deletion in *nestin*-expressing progenitors of the adult brain affected hippocampal adult neurogenesis by affecting the early proliferating progenitor population. Therefore, we next investigated the effects of *Tcf4* deletion in the proliferating neural progenitor cells (NPC). To understand the cell-intrinsic effects in NPC while avoiding potential secondary effects from its niche, we isolated hippocampus from the WT and KO brains for neurosphere cultures and induced *Tcf4* deletion in progenitors in culture.

Consistent with the in vivo data demonstrating reduction in $BrdU^+$, $Ki67^+$, $Sox2^+$, and $Tbr2^+$ cells in KO DG, the *Tcf4*-deleted progenitors formed significantly smaller number of neurospheres (Fig. 5A), which were also smaller in size (Fig. 5B and fig. S4A), indicating loss of proliferative capacity. Furthermore, the KO neurospheres often exhibited spreading (Fig. 5B) and did not give rise to secondary neurospheres (Fig. 5C and fig. S4B), indicating loss of self-renewal capacity.

To elucidate the molecular effect of *Tcf4* deletion in neural progenitors, we performed RNA sequencing (RNA-seq) analysis of NPC from neurospheres, which showed 740 differentially regulated genes (DEGs) between WT and Tcf4-KO NPC (fig. S8). Unexpectedly, the transcriptomic data revealed that *Tcf4* deletion in hippocampal proliferating progenitors resulted in an up-regulation of myeloid inflammatory gene signature in the NPC, with Lgals3 (Galectin-3) and CD68 being two of the top up-regulated genes (Fig. 5D and fig. S4C). We further confirmed protein expression of Lgals3 (Fig. 5E) and CD68 (fig. S4, E and F), in genetically traced (GFP+ve) WT and KO progenitors. Lgals3 is a gene implicated in inflammatory process in multiple tissues, including the brain (*36*–*38*), and CD68 is a prominent lysosomal marker expressed by myeloid cells. Expression of these proteins in the *Tcf4*-deleted progenitors further confirmed their myeloid inflammatory transformation. Last, analysis of gene ontology of the top 50 significantly up-regulated genes in KO progenitors identified "inflammatory response" and "extracellular matrix organization" as the prominent up-regulated functions of the KO progenitors (Fig. 5F and tables S1 and S5). Conversely, cell cycle and neuronal differentiation pathways were down-regulated in the KO progenitors (Fig. 5D; fig. S4, C and D; and tables S2 and S6). Given the up-regulation of myeloid and inflammatory genes in KO progenitors, we further performed a meta-analysis from publicly available myeloid gene sets (*39*, *40*), wherein the genes known to identify "myeloid cells" were plotted for their expression level in our NPC RNA-seq dataset for cumulative frequency distribution analysis. As shown in Fig. 5G, the myeloid gene sets showed a clear up-regulation in *Tcf4*-KO progenitors. These data show that *Tcf4* deletion in *nestin*-expressing progenitors leads to their transformation into a myeloid inflammatory cell state.

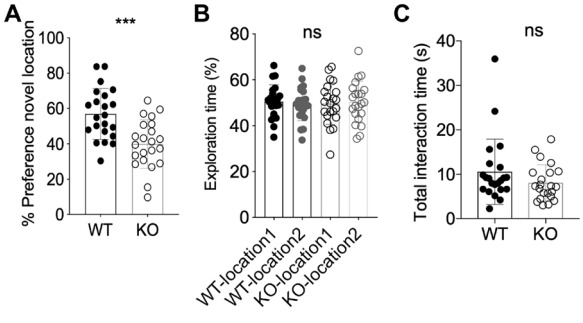

Fig. 4. Tcf4 deletion in adult NSC causes deficit in the NLR memory task. (**A**) NLR performance of WT and KO animals. (**B**) Exploration during training demonstrating no inherent bias for either location. (**C**) Total interaction time during test showing no deficit in movement or exploration for WT or KO animals. $n = 22$ animals per genotype, each dot represents an animal. Error bar represents SD. Mann-Whitney test was done for statistical analysis. ***$P = 0.0004$, ns, nonsignificant.

Tcf4-deleted hippocampal neural progenitors show aberrant differentiation potential

Given the spread-out morphology in KO neurospheres, we also examined the differentiation potential of the NPCs in the absence of Tcf4. Consistent with the transcriptome data (Fig. 5D), the KO progenitors indeed showed aberrant differentiation, expressing the neuronal marker Tuj1 along with the oligodendrocyte gene myelin-basic protein (MBP) and the myeloid gene CD68, two of the top up-regulated genes detected in RNA-seq of the KO progenitors (Fig. 6, A to D). Furthermore, differentiated KO progenitors presented a stalky morphology when compared with the thin long processes seen in the differentiated WT progenitors (Fig. 6, A and B, and fig. S5B).

Since the KO progenitors showed up-regulation of a number of myeloid genes, including CD68 which is also expressed by the brain-resident myeloid cell microglia, we examined whether the KO progenitors were adopting microglial cell fate. For this, we investigated coexpression of the microglial marker Iba1 in *nestin*-expressing progeny by in vivo genetic lineage tracing, which showed that the *Tcf4*-deleted NPC do not give rise to microglia (fig. S5). This is consistent with our transcriptome data that showed that while inflammatory and myeloid genes were up-regulated in the KO progenitors, core microglia genes such as SiglecH and Sall1, were not. Together, the differentiation and lineage tracing investigations of NPC confirmed that *Tcf4* deletion renders the hippocampal proliferative progenitors in an aberrant state, with up-regulated myeloid inflammatory genes and faulty differentiation outcome.

Tcf4 deletion in adult neural progenitors causes inflammation in the DG

Given the rather unexpected myeloid inflammatory transformation of hippocampal NPC upon *Tcf4* deletion, we wanted to confirm this

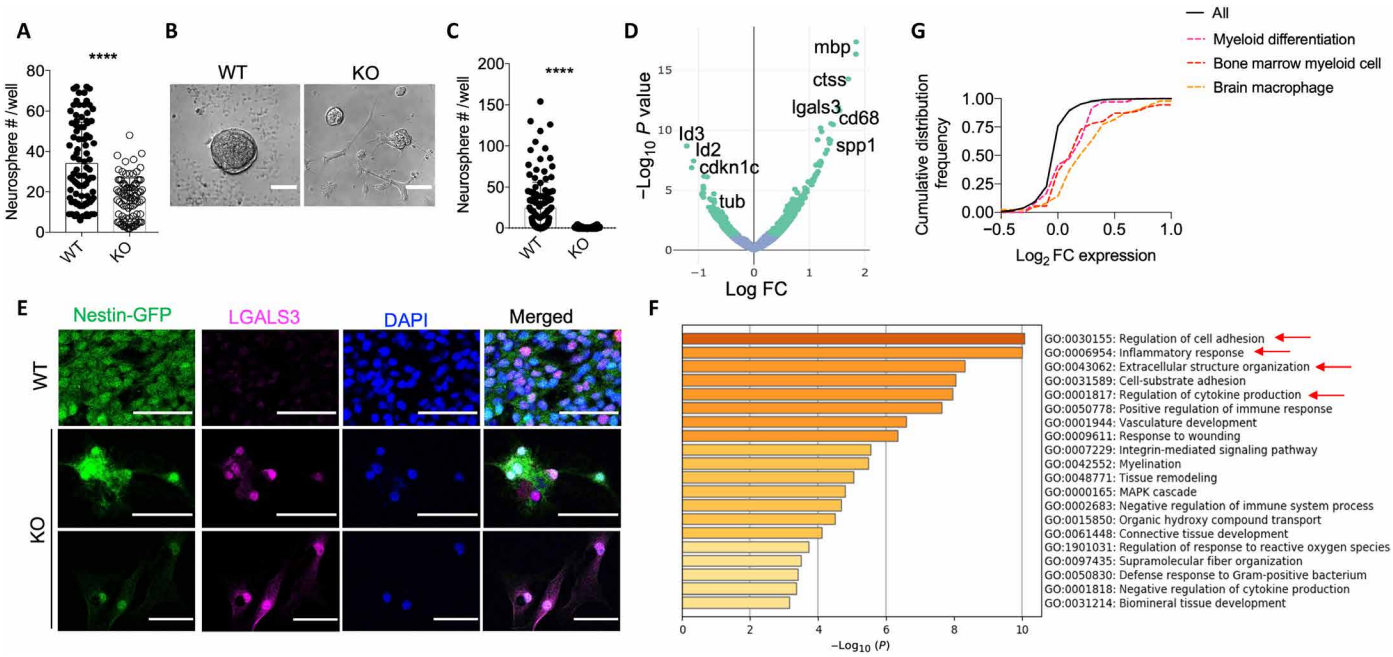

Fig. 5. Tcf4-deleted neural progenitors gain myeloid inflammatory potential. (**A**) Neurosphere counts from WT and Tcf4-deleted hippocampal progenitors (NPC) (each dot represents neurosphere counts per well from three brains per genotype). (**B**) Representative neurosphere phenotype. (**C**) Secondary neurosphere counts; $n = 3$ mice per genotype; error bar represents SD, $P < 0.0001$. (**D**) Volcano plot showing differentially expressed genes in WT versus KO neurospheres, ($P < 0.05$, green dots). FC, fold change. (**E**) Representative images of genetically traced (GFP$^+$) WT and KO NPC for the expression of LGALS3. Scale bars, 50 μm. (**F**) Enriched ontology cluster analysis for the top 50 up-regulated genes in KO progenitors. (**G**) Cumulative frequency distribution curve showing up-regulation of "myeloid" gene sets in KO progenitors' transcriptome. MAPK, mitogen-activated protein kinase.

in vivo. However, because of the very low numbers of stem and progenitor population in the adult SGZ, we were not able to sort enough viable cells from the DG for analysis. This could also be because, as seen in neurosphere cultures, the KO progenitors showed poor proliferation as depicted by smaller size and loss of self-renewal. Therefore, to confirm the in vivo presence of the inflammatory transformation of NPC upon *Tcf4* deletion, we reasoned that if indeed the Tcf4-deleted progenitors turn inflammatory in vivo, there should be inflammation in the SGZ niche. To examine this in an unbiased manner, we induced *Tcf4* deletion in *nestin*-expressing progenitors in WT and KO animals and microdissected the SGZ niche (DG) to perform transcriptome analysis, which showed 462 DEG between WT and *Tcf4*-KO DG (fig. S9). Consistent with our hypothesis, the KO DG indeed showed up-regulation of genes typically involved in immune and inflammatory responses, such as lysozyme2 and several IFN response genes (Fig. 7A and fig. S6A), as a result of *Tcf4* deletion in *nestin*-expressing progenitors. Consistently, the enriched ontology analysis of the top 50 significantly up-regulated genes in the KO-DG showed IFN response as the top up-regulated functional pathway (Fig. 7B and tables S3 and S7). Conversely, the neuronal signaling pathways were down-regulated in the KO DG (fig. S6B and tables S4 and S8) indicating detrimental effects of inflammation on hippocampal function.

To further confirm inflammation in KO brain DG, we examined microglial activation, a hallmark indicator of parenchymal inflammation, as demonstrated by CD68 up-regulation in microglia. Consistent with inflammatory gene signature of the KO-DG, microglia in the KO brains showed higher CD68 expression (Fig. 7, C and D, and fig. S6C), confirming microglial response to inflammation. We also investigated cell death in DG by TUNEL staining, to rule out increased cell death as a possible cause of inflammation in the KO DG. As shown in fig. S7 (A and B), there was no difference in cell death between the WT and KO DG.

Tcf4-deleted neural progenitors produce detrimental factors that adversely affect niche cells

The correlative evidence for inflammatory gene expression of *Tcf4*-KO progenitors (Fig. 5) and the presence of inflammation in the KO brain DG (Fig. 7) suggested that the KO progenitors may produce factors that could cause inflammation in DG. To confirm that *Tcf4*-deleted progenitors could indeed adversely affect its niche cells, including the possibly undeleted NPC in KO brain SGZ, we designed a coculture experiment using *nestinCreER-Tcf4 flox; flox*-STOP-*flox*-EGFP brains for neurosphere cultures. For this, we induced *Tcf4* deletion in progenitors from KO brain DG in only half of the progenitors, while the other half was vehicle-treated to mimic undeleted progenitors in the KO-DG (reported as WT for this experiment). We adopted this coculture regime after validating that tamoxifen treatment does not have its own nonspecific effect on NPC, by comparing neurospheres from tamoxefin-treated WT with vehicle-treated *Tcf4-flox* progenitors, which showed no difference in either genotype or phenotype (fig. S7, C and D).

Once the KO neurospheres appeared green because of *Cre*-induced recombination and GFP expression (while vehicle-treated controls remained GFP$^+$; labeled as WT for this experiment), WT and KO progenitors were put together in a single well for coculture to investigate the effect of KO progenitors on its neighboring cells. The vehicle-treated *Tcf4*-flox progenitors (WT) and the tamoxifen-treated

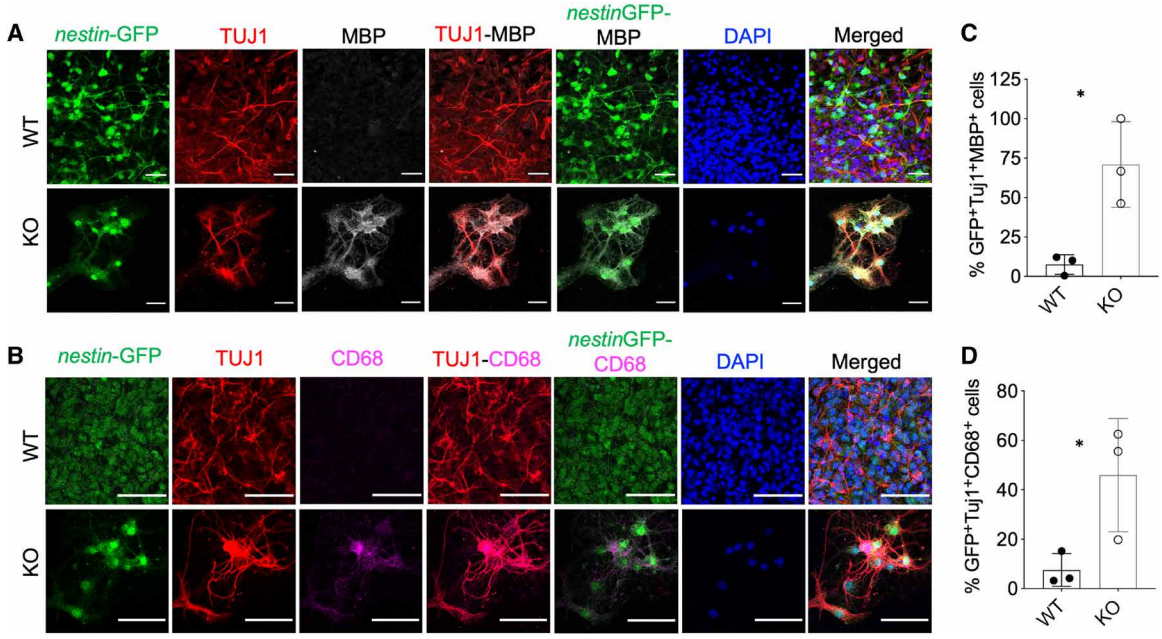

Fig. 6. Tcf4-deleted hippocampal neural progenitors show aberrant differentiation potential. (**A** and **B**) Representative image for differentiation phenotype of neural progenitors, demonstrating coexpression of neuronal gene Tuj1 and oligodendrocyte gene MBP (A) and Tuj1 and myeloid gene CD68 (B) in genetically traced GFP$^+$ Tcf4-deleted KO progenitors. (**C** and **D**) Quantification of percentage of aberrant cells among the lineage traced progenitors. Each dot represents average counts from an animal; error bars represent SD. *$P < 0.05$. Scale bars, 50 μm.

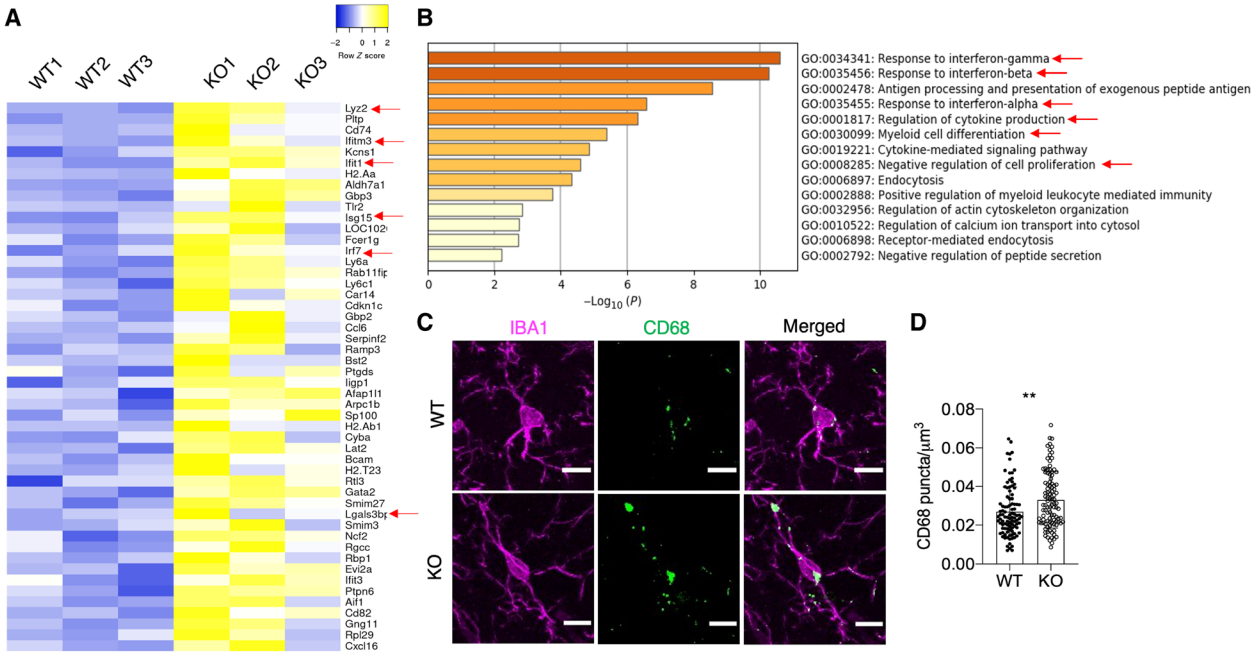

Fig. 7. Tcf4 deletion in neural stem cells cause inflammation in the DG. (**A** and **B**) Heatmap (A) and enriched ontology cluster analysis (B) of the top 50 up-regulated genes in the DG of KO brains. (**C**) Representative images of microglia in WT and KO-DG. (**D**) CD68 puncta counts from (C). (**$P = 0.007$, three brains per genotype; error bar represents SD). Scale bars, 10 μm.

Tcf4-flox progenitors (KO) are shown as control from the same brain (Fig. 8A, left). The hydroxy-tamoxifen (OH-Tmx)–induced GFP expression in KO progenitors allowed us to discern the *Tcf4*-undeleted (WT) progenitors from the *Tcf4*-deleted (KO) progenitors in the same well. As shown in Fig. 8A, the health of the WT neurospheres (white arrows) was severely compromised when cocultured with KO progenitors (green arrows) in the same well, indicating that *Tcf4*-deleted progenitors not only have a cell-intrinsic

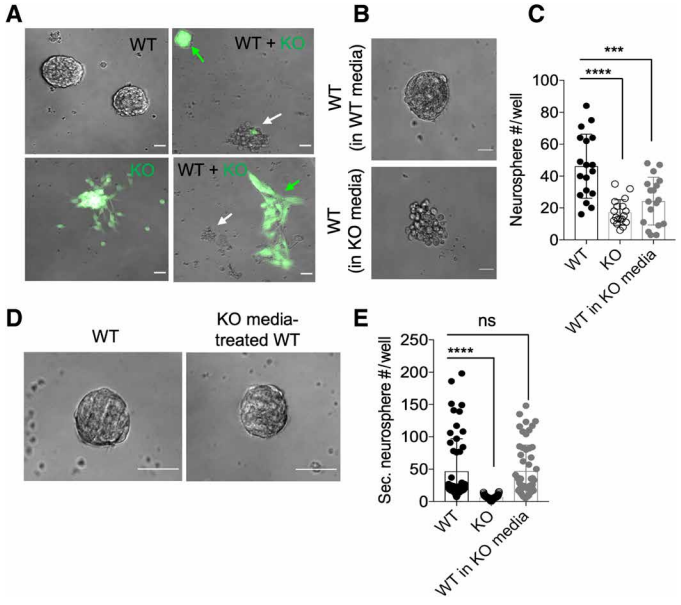

Fig. 8. *Tcf4*-deleted neural progenitors produce detrimental factors that adversely affect niche cells. (**A**) Representative neurosphere images from WT, KO, and WT-KO cocultures. Green arrows show *Tcf4*-deleted neurospheres, and white arrows show WT neurosphere in coculture wells. (**B**) Representative images showing WT neurospheres in normal media versus in media from KO cultures. (**C**) Neurosphere counts from (B). (**D**) Representative secondary neurosphere images demonstrating recovery of KO media–treated WT neurospheres when returned backed to normal media. (**E**) Neurosphere counts of (D). Three brains per genotype; error bar represents SD (****$P < 0.0001$ and ***$P = 0.0007$). Scale bars, 50 μm.

detrimental effect on themselves but also have a detrimental effect on its neighboring cells.

Lastly, to test whether the influence of KO progenitors is possibly through extracellular/secreted factors, we separately cultured progenitors from WT and KO brains treated with OH-Tmx. We then transferred the culture media from the KO neurospheres onto the WT neurospheres, to examine potential adverse effects of secreted factors from KO-NPC on WT progenitors. This indeed resulted in deterioration of the health and number of the WT neurospheres (Fig. 8, B and C). However, the adverse effect of KO neurosphere media on WT progenitors was reversible, since upon returning to normal media, the WT progenitors were rescued from "unhealthy" phenotype and formed neurospheres that were normal in morphology and numbers, comparable to WT neurospheres in normal media (Fig. 8, D and E). We also examined whether cell death and related factors in KO NPC culture could be responsible for the adverse effects of KO media–secreted factors. For this, we performed cleaved–caspase-3 staining of the neurosphere cultures, which showed no cell death in WT or KO neurosphere cultures (fig. S7C). In contrast, as a positive control, the etoposide-treated cultured cells showed positive staining for cleaved caspase-3 (fig. S7D). This further confirmed that the genetic deletion of *Tcf4* in hippocampal NPCs also has a "cell-extrinsic" effect manifested through the production of extracellular factors by the KO progenitors, which could adversely influence its niche cells. This is in addition to the "cell-intrinsic" effects of *Tcf4* deletion in NPC that is manifested as its myeloid transformation, affecting the progenitors' proliferation and differentiation potential (as shown in Figs. 5 and 6).

DISCUSSION

The neural stem cells of the adult brain have been characterized in detail with regard to their transcriptome and proteome in recent years, thereby detailing molecular regulations that underlie adult NSC maintenance (*41*, *42*), differentiation, and fate potential (*43*, *44*). Specifically, studies examining the potential of the adult hippocampal progenitors have revealed that the fate of these progenitors is restricted to neuron, astrocyte, and oligodendrocyte lineages with a bias toward neuronal differentiation (*45*, *46*).

Investigating the functional relevance for the high expression of a cell fate regulatory transcription factor *Tcf4* in the adult neurogenic niche, we have uncovered an unexpected aspect of the adult NSC. Our study reveals that *Tcf4*, which is highly expressed in the adult neurogenic cells, facilitates hippocampal adult neurogenesis by proactively suppressing an inflammatory potential of the neural progenitors. Transcriptome analysis of *Tcf4* deleted *nestin*-expressing neural progenitors revealed that a number of genes that are known to be expressed in myeloid cells, such as *Ctss*, *Mpeg1*, *Lgals3*, *CD68*, and *Spp1* are up-regulated in neural progenitors upon *Tcf4* deletion, indicating their transformation into a myeloid inflammatory state. *Lgals3* is highly expressed by a variety of myeloid cells including macrophage and neutrophils and has been implicated in immunemodulatory functions including chemotaxis and extracellular matrix regulation (*47*, *48*). Corresponding to the up-regulation of *Lgals3* in KO NPC, its binding partner Lgals3bp was up-regulated in the KO brain DG, as shown in transcriptomic datasets. Consistent with the myeloid inflammatory gene signature of the KO progenitors, we were able to detect protein expression of the inflammatory gene Lgals3 and the lysosomal marker CD68, both of which are known to be expressed in myeloid cells, in the KO progenitors. As expected, we observed that the myeloid inflammatory transformation of the KO progenitors resulted in inflammation in the KO DG, depicted by an up-regulation of IFN response gene signature. Consistent with this, we further confirmed that the KO progenitors indeed produce extracellular factors that detrimentally affect its niche cells.

Together, our observations demonstrate that *Tcf4* deletion in aNSC adversely affects the process of adult neurogenesis in two ways; on one hand, it abolishes the proliferative and differentiation capacity of the NPC, while on the other hand, it causes inflammation in the niche via the NPCs' inflammatory transformation. Given that inflammation is already known to adversely affect mammalian adult neurogenesis (*7*–*10*), the inflammatory transformation of adult NPC likely affects adult neurogenesis further in the KO brain. This two-pronged effect of *Tcf4* deletion in adult NSC can be understood as a cell-intrinsic effect that leads to abolition of the neuronal fate potential by transforming the progenitors into a myeloid-like inflammatory cell state and a cell extrinsic effect due to production of detrimental factors as a result of their transformation, thereby further affecting the niche cells.

The importance of *Tcf4* in the CNS is underscored by its implication in neurodevelopmental (PTHS) as well as psychiatric (SCZ) disorders. While a number of studies have demonstrated the role for *Tcf4* in brain development and embryonic neural stem cells, the underlying mechanism and targets of *Tcf4* in the embryonic brain remain poorly understood. Furthermore, *Tcf4*'s role in the postnatal brain, where it continues to be abundantly expressed, has only started to emerge, implicating *Tcf4* in myelination (*19*) and neuronal activity (*23*, *49*–*51*). However, *Tcf4*'s potential function in the adult neural stem cell remains unexplored. It is important to note that

new transcriptomic dataset of the adult hippocampal NSC reveals that the adult NSC diverge from the embryonic NSC at a very early postnatal stage, around postnatal day 5-7 (*45*). Given this, the molecular regulators and the possibilities of fate potential for adult NSC are likely to be different from the embryonic NSC, especially given the environment-responsive functions of adult hippocampal NSC. In this regard, our study reveals a completely unprecedented aspect of adult NSC, its latent myeloid inflammatory potential, and implicates Tcf4 in suppression of this detrimental potential.

Injury-induced neurodegeneration and inflammation have been shown to induce NSC proliferation and neurogenesis in zebrafish (*52*). However, a quest for similar response in mammalian model systems has largely met with disappointment. Analysis of human samples from neurodegenerative disorders such as Huntington's disease (*53*) and Alzheimer's disease (AD) (*54*) demonstrates a decline in adult neurogenesis under neurodegenerative conditions. Since parenchymal inflammation is known to be concomitant in these neurodegenerative diseases, this further emphasizes that the mammalian adult brain NSC respond adversely to inflammation. However, the source of inflammation and its potential molecular link to reduction in adult neurogenesis remain unclear. Our observations provide the first evidence that (i) inflammation can be triggered cell intrinsically by adult neural progenitors residing in the DG and (ii) that *Tcf4* is a cell-intrinsic regulator of aNSC that proactively suppresses the inflammatory potential of aNSC, to facilitate normal adult neurogenesis.

The revelation of a latent inflammatory potential of the adult NSC may have broader implications beyond the field of adult neurogenesis, in the wider context of aging, neurodegeneration, neuroinflammation, and regenerative approaches where all the effectors are not yet fully understood. For instance, although adult neurogenesis is known to decline with age, what triggers the aging NSCs to adopt quiescence remains poorly understood. Whether aging RGL adopt an inflammatory state that affects their functions remain elusive. In the context of regenerative research, the potential of neural stem cell is considered to be only CNS-friendly neural cells; however, the presence of a latent inflammatory property within these cells would be a critical aspect to keep in consideration. In the case of neurodegenerative disorders, while a reduction in adult neurogenesis is observed at the very early stages of AD (*54*), the triggers for the degenerative process in AD remain unknown. A potential involvement of a CNS-intrinsic trigger for inflammatory processes contributing to neuroinflammation and neurodegeneration would be an important question to explore. Our observations provide evidence that adult NSC residing in the hippocampus harbors an inflammatory potential that is proactively suppressed, thereby shedding light on to a previously unknown potential source of inflammation within CNS. However, future studies identifying potential physiological contexts for the inflammatory transformation of aNSC will be needed to provide further insights into the physiological and clinical relevance of our findings.

MATERIALS AND METHODS

Mice

All animals were housed, bred, and used according to the protocols approved by the Institutional Animal Care and Ethics Committee. The *Nestin-Cre^{ERT2}* transgenic line (*1*) was a gift from R. Hen, Columbia University Medical Center, New York, USA. For conditional targeting of Tcf4 in *Nestin*-expressing progenitors in the adult brain, Tcf4-flox line (*27*, *55*) was crossed with *Nestin-Cre^{ERt2}* line to produce *Nestin-Cre^{ERt2}; Tcf4f/f* (KO) or *Nestin-Cre^{ERt2}; Tcf4+/+* (WT). For genetic lineage tracking, the flox-STOP-flox-EGFP reporter from The Jackson Laboratory (strain 32037-JAX) was further crossed on to *NestinCre^{ERt2}*; *Tcf4* flox/wt line. All animals were bred and kept at the Animal Care and Resource Centre.

Mice treatments

Tamoxifen (Sigma-Aldrich) was used at 5 mg/35 g body weight once a day for 4 days for *Nestin*-Cre induction in WT and KO adult animals at the age of P45-60. For BrdU pulse-chase experiment, mice were given BrdU (Sigma-Aldrich) in drinking water at 1 mg/ml concentration for 7 days or five intraperitoneal injections/day for 5 days, followed by 14 days or 6 days of chase, respectively, before euthanizing animals for analysis. For genetic lineage tracing experiment, tamoxifen treatment was used to induce the EGFP expression and Tcf4 deletion, and mice were euthanized at 7, 11, 30, or 60 days after tamoxifen treatment for various time point analysis.

Immunostaining

Animals were deeply anesthetized and transcardial perfusion with phosphate-buffered saline, followed by 4% paraformaldehyde (PFA) was done. Brains were kept in PFA for overnight fixation at 4°C, and 30-μm sections were sliced using vibratome. For immunostaining, floating sections were first blocked [10% normal goat serum, 1% bovine serum albumin (BSA), 0.1% Triton X-100, and 100 mM glycine] for 1 hour at room temperature(RT) and stained with primary antibody (in 1% normal goat serum, 0.1% BSA, 0.1% Triton, and 100 mM glycine) overnight at 4°C. Sections were then washed and incubated with fluorophore-conjugated secondary antibody for 1 hour at RT in dark, before mounting and imaging. Primary antibodies used were DCX (Millipore #2253 and Abcam #18723), BrdU (AbD Serotec #MCA2060T), Calbindin (SySy #214005), Prox1 (Millipore #5654), Tbr2 (Abcam #23345 and Invitrogen #14-4875-82), glial fibrillary acidic protein (Invitrogen #130300), CD68 (AbD Serotec #MCA1957), Tcf4 (Abcam #217668), Ki67 (eBioscience #14-5698-82 and Abcam #ab16667), Lgals3 (Invitrogen #50-5301-80), MBP (SySy #295004), Tuj1 (Promega #G7121), Iba1 (SySy #234006), CD68 (AbD Serotec #MCA1957), and cleaved caspase-3 (Cell Signaling Technology #9664). Tunel assay was performed as per the manufacturer's instructions (Roche/Sigma-Aldrich, 12156792910).

Confocal imaging and analysis

Sections were imaged using a Leica SP8 confocal microscope at 63×, 40×, or 20× objective. Images were analyzed using Fiji and Imaris. For cell number quantitation in Fiji, individual cells of interest were marked as region of interest (ROI) by going through the Z-stacks of individual images. The cell numbers were then normalized with the area of DG blades for that section, as marked using Fiji ROI function. For Imaris analysis, the surface and spot modules were used for counts and intensity measurements. At least three to four sections from each mouse were analyzed, and least three to five mice per genotype/group for each experiment were used. For counts per animal, the counts from each slice of an animal were averaged and presented as the count for that animals. For absolute counts per DG, sections every 180th micron rostrocaudally throughout the DG were counted and multiplied by six to estimate counts from entire DG. For neurosphere cultures, cells were quantified from multiple

images from individual animal's neurosphere culture and plotted as percentage of GFP+ve cells. For altered morphology quantification, well-separated GFP$^+$ Tuj1$^+$ cells whose primary process could be properly identified to mark as stalky were counted. Unpaired Student's *t* test was used for statistical analysis for all immunofluorescence-based quantification.

Neurosphere culture

For neurosphere culture of progenitors from tamoxifen-treated *Nestin-Cre^{ERt2}/TCF4$^{fl/ff\ or\ wt}$* adult animals, the hippocampus was harvested 1 month after tamoxifen induction in the animals. The tissue was digested in 0.05% trypsin-EDTA, filtered through a 70-μm sieve, and seeded as 5000 cells per well in a 96-well plate in neurobasal growth media with B27 and GlutaMAX supplement, recombinant mouse epidermal growth factor (EGF) (20 ng/ml), and recombinant mouse fibroblast growth factor (FGF-2) (20 ng/ml). Neutrospheres were counted at day in vitro (DIV14). For in vitro deletion and functional assays, *Nestin-Cre^{ERt2}/TCF4$^{fl/ff\ or\ wt}$* brains of P10-13 mice were used, since the number of neurospheres obtained from 2- to 3-month-old mouse brain was very limiting. The use of P10-13 brains for neurosphere cultures was justified on the basis of recent transcriptomic revelation (*45*) establishing that neural progenitors from P5 to adulthood cluster together as one group with regard to their transcriptome. We adapted previously published protocol (*56*) for hippocampal neurosphere culture as follows: Hippocampi from individual brains were microdissected and digested in PDD [papain (2.5 U/ml), Dispase II (1U/ml), and deoxyribonuclease I (10 μg/ml)] for 30min in a shaker incubator at 37°C and 170 rpm with intermittent trituration. The digestion was stopped by adding complete neurobasal media (neurobasal supplemented with B27, GlutaMAX, and anti-anti). The cell suspension was strained through a 40-μm sieve and washed in wash buffer (30 mM glucose, 2 mM Hepes, and 26 mM $NaHCO_3$ in 1× Hanks' balanced salt solution) by centrifuging cells at 130*g* for 5 min at 21°C. The cell pellet was resuspended in 20 ml of complete neurobasal media, along with EGF and FGF (20 ng/ml), and seeded in a flat-bottom 96-well plate. For *Cre*-induced deletion in neurosphere cultures, 0.5 μM 4-OH-Tmx (Sigma-Aldrich) was added in cell suspension at the time of seeding. The cells were incubated in a tissue culture (TC) incubator with 5% CO_2 for 5 to 10 days. Neurospheres were counted at DIV7 and presented as counts per well for each brain. For immunofluorescence studies, neurospheres were transferred on poly-D-lysine–coated sterile coverslips in a 24-well plate and incubated for 48 hours in neurosphere growth media. The cells were then fixed in 4% PFA for 15 min at RT and stained.

Secondary neurosphere

For the secondary neurosphere culture, primary neurospheres were collected and spun down at 200*g* for 10 min. The cell pellet was then gently triturated in neurosphere growth media using a 200-μl tip. The single-cell suspension was then spun down and resuspended in fresh neurosphere growth media supplemented with growth factors and seeded into a fresh 96-well plate. Secondary neurospheres were counted at DIV5.

Differentiation of neurosphere

Neurospheres were gently triturated to make single-cell suspensions as stated above. The single-cell suspension was then plated on poly-D-lysine–coated sterile coverslips in a 24-well plate. After 1 hour of incubation in the TC incubator, when the cells had adhered on to the coverslip, the medium was replaced with fresh differentiation medium without the growth factors EGF/FGF. The differentiation culture was allowed to grow for 3 days in the TC incubator. Cell were fixed at DIV3 in 4% PFA for 15 min at RT and stained for immunofluorescence studies.

Coculture experiments

For coculture experiments, cultures from *Nestin-Cre^{ERt2}/TCF4$^{fl/fl}$* brains, with or without OH-Tmx, were used for detection of WT and KO neurospheres when cocultured in the same well, on the basis of tamoxifen-induced GFP expression only in KO. First, the neurospheres cultures were allowed to grow until DIV6 with (KO) or without OH-Tmx (WT). At this point, the OH-Tmx–treated wells showed GFP+ve neurospheres, whereas the vehicle-treated were not GFP+ve. The neurospheres were then gently collected in a tube and centrifuged at 130*g* for 5 min in culture media for wash. The cell pellets from WT and KO tubes were then resuspended very gently in fresh media, so as to not dissociate the spheres, and seeded together for coculture. Cocultured WT and GFP-expressing KO neurospheres were counted and imaged 2 days after the coculture was set up. WT and KO neurospheres in "no-mix/pure" culture wells were used as controls. The number and morphology of neurospheres in the cocultures were compared with "pure"-cultured WT neurospheres in the same experiment.

Media swap experiments

Brains from *Nestin-Cre^{ERt2}/TCF4$^{fl/fl}$ and Nestin-Cre^{ERt2}/TCF4^{wt}* mice were cultured with OH-Tmx as described above, except that each brain was seeded in 12 wells of a 24-well plate. On DIV6 to DIV7, neurospheres from six WT wells and six KO wells were gently collected in a tube and spun down at 200*g* for 10 min. The supernatant was collected in a fresh tube and labeled as WT or KO media. The KO media was then used to resuspend the WT neurosphere pellet and the WT media used for KO neurospheres. The transfer and resuspension were done very gently using a 200-μl tip to avoid dissociation of neuropsheres. The neuropsheres with exchanged media were then seeded into a fresh 24-well plate, so as to avoid effects of any residual media from the original cultures. For comparison of neurospheres in exchanged media with those in the original media, controls from the same experiment were used. For this, the remaining six WT wells' and six KO wells' neurospheres were similarly collected and spun down but resuspended in their own media. These were then plated in the same fresh 24-well plate as the "exchanged media" neurospheres. All the replated neurospheres were allowed to grow for 48 hours, after which they were counted and imaged for analysis. Furthermore, the WT, KO, and "media-exchanged"-WT neurospheres were put for secondary neurosphere culture in fresh neurosphere growth media to examine whether the affected WT neurospheres treated with KO neurosphere media were able to recuperate when put back in normal media.

RNA sequencing

RNA was isolated from neurospheres and microdissected DG of individual mice, using a Qiagen Micro Plus kit as per the manufacturer's instructions. Sample quality control, library preparation, and RNA-seq were done by the Next-Generation Sequencing facility at the institute. RNA quality was assessed using the Bioanalyzer. cDNA libraries were prepared by using New England Biolabs stranded mRNA

library prep kit as per the manufacturer's instructions. PolyA selection method was used to enrich mRNA. Library quality was analyzed with the Bioanalyzer. Next-generation sequencing of libraries was performed at the Next-Generation Sequencing facility at the institute on the Illumina HiSeq 2500 platform for 1 × 100 bp at ~20 to 25 million reads per sample.

RNA-seq data analysis

The public server at usegalaxy.org was used to analyze the sequencing data. Briefly, after cutting the adapter sequence and initial quality check for sequence reads, Hisat2 was used to align the reads to *Mus musculus* mm10 reference genome, and feature counts were generated. For differential gene expression, the DESeq2 tool was used, and the output was annotated using "annotateMyID" feature in Galaxy. This differential gene expression output was used for volcano plot using R. Normalized feature counts were used to plot heatmap using the web tool "heatmapper." Enriched ontology cluster analysis was done using the public web tool at metascape.org (*57*).

NLR test

The animals were housed in individually ventilated cages with easy access to food and water with 14 hours of light and 10 hours dark cycles, respectively. Before the start of experiment, animals were individually handled for 5 min for 3 days. On day 1, animals were acclimatized with the arena in which experiment was to be performed. For this, the animals were released individually in arena for 5 min and then placed back into home cages. On training day (day 2), two identical objects were placed in the box near a wall with a triangular black sticker used as a visual anchor. The training was performed for 10 min, where animals were released individually into the arena in the corner of wall opposite to the objects and allowed to explore the objects freely for 10 min. After training, animals were placed back into their home cages. On the test day (day 3), one of the two objects were displaced to a new location (novel location) with respect to the previous location. The animal was then reintroduced in the arena as during training session and allowed to explore the objects for 5 min. NLR was done 9 to 11 days after tamoxifen treatment. The training and test sessions were recorded with top head camera, and the videos were manually analyzed for exploration time at each object as a proxy for location recognition. The time spent exploring the old versus newly located object was calculated. For this, the time spent in active sniffing of the object was taken as exploration. Rearing with head above the object level and climbing onto the object were not counted as "exploration." Percentage exploration was calculated as (time spent on one object/total time spent on both objects) × 100. Statistical analysis was done using Mann-Whitney test.

SUPPLEMENTARY MATERIALS

Supplementary material for this article is available at http://advances.sciencemag.org/cgi/content/full/7/21/eabf5606/DC1

View/request a protocol for this paper from *Bio-protocol*.

REFERENCES AND NOTES

1. A. Dranovsky, A. M. Picchini, T. Moadel, A. C. Sisti, A. Yamada, S. Kimura, E. D. Leonardo, R. Hen, Experience dictates stem cell fate in the adult hippocampus. *Neuron* **70**, 908–923 (2011).
2. H. Van Praag, G. Kempermann, F. H. Gage, Running increases cell proliferation and neurogenesis in the adult mouse dentate gyrus. *Nat. Neurosci.* **2**, 266–270 (1999).
3. G. Kempermann, H. G. Kuhn, F. H. Gage, More hippocampal neurons in adult mice living in an enriched environment. *Nature* **386**, 493–495 (1997).
4. C. Mirescu, J. D. Peters, E. Gould, Early life experience alters response of adult neurogenesis to stress. *Nat. Neurosci.* **7**, 841–846 (2004).
5. C. L. Coe, M. Kramer, B. Czéh, E. Gould, A. J. Reeves, C. Kirschbaum, E. Fuchs, Prenatal stress diminishes neurogenesis in the dentate gyrus of juvenile rhesus monkeys. *Biol. Psychiatry* **54**, 1025–1034 (2003).
6. V. Lemaire, M. Koehl, M. Le Moal, D. N. Abrous, Prenatal stress produces learning deficits associated with an inhibition of neurogenesis in the hippocampus. *Proc. Natl. Acad. Sci. U.S.A.* **97**, 11032–11037 (2000).
7. M. L. Monje, H. Toda, T. D. Palmer, Inflammatory blockade restores adult hippocampal neurogenesis. *Science* **302**, 1760–1765 (2003).
8. C. T. Ekdahl, J. H. Claasen, S. Bonde, Z. Kokaia, O. Lindvall, Inflammation is detrimental for neurogenesis in adult brain. *Proc. Natl. Acad. Sci. U.S.A.* **100**, 13632–13637 (2003).
9. S. A. Villeda, J. Luo, K. I. Mosher, B. Zou, M. Britschgi, G. Bieri, T. M. Stan, N. Fainberg, Z. Ding, A. Eggel, K. M. Lucin, E. Czirr, J.-S. Park, S. Couillard-Després, L. Aigner, G. Li, E. R. Peskind, J. A. Kaye, J. F. Quinn, D. R. Galasko, X. S. Xie, T. A. Rando, T. Wyss-Coray, The ageing systemic milieu negatively regulates neurogenesis and cognitive function. *Nature* **477**, 90–94 (2011).
10. L. Katsimpardi, N. K. Litterman, P. A. Schein, C. M. Miller, F. S. Loffredo, G. R. Wojtkiewicz, J. M. Chen, R. T. Lee, A. J. Wagers, L. L. Rubin, Vascular and neurogenic rejuvenation of the aging mouse brain by young systemic factors. *Science* **344**, 630–634 (2014).
11. H. Yousef, C. J. Czupalla, D. Lee, M. B. Chen, A. N. Burke, K. A. Zera, J. Zandstra, E. Berber, B. Lehallier, V. Mathur, R. V. Nair, L. N. Bonanno, A. C. Yang, T. Peterson, H. Hadeiba, T. Merkel, J. Körbelin, M. Schwaninger, M. S. Buckwalter, S. R. Quake, E. C. Butcher, T. Wyss-Coray, Aged blood impairs hippocampal neural precursor activity and activates microglia via brain endothelial cell VCAM1. *Nat. Med.* **25**, 988–1000 (2019).
12. S. A. Wolf, B. Steiner, A. Akpinarli, T. Kammertoens, C. Nassenstein, A. Braun, T. Blankenstein, G. Kempermann, CD4-Positive T lymphocytes provide a neuroimmunological link in the control of adult hippocampal neurogenesis. *J. Immunol.* **182**, 3979–3984 (2009).
13. H. Zhang, B. Shao, Q. Zhuge, P. Wang, C. Zheng, W. Huang, C. Yang, B. Wang, D. M. Su, K. Jin, Cross-talk between human neural stem/progenitor cells and peripheral blood mononuclear cells in an allogeneic co-culture model. *PLOS ONE* **10**, e0117432 (2015).
14. Y. Ziv, N. Ron, O. Butovsky, G. Landa, E. Sudai, N. Greenberg, H. Cohen, J. Kipnis, M. Schwartz, Immune cells contribute to the maintenance of neurogenesis and spatial learning abilities in adulthood. *Nat. Neurosci.* **9**, 268–275 (2006).
15. L. Möhle, D. Mattei, M. M. Heimesaat, S. Bereswill, A. Fischer, M. Alutis, T. French, D. Hambardzumyan, P. Matzinger, I. R. Dunay, S. A. Wolf, Ly6Chi monocytes provide a link between antibiotic-induced changes in gut microbiota and adult hippocampal neurogenesis. *Cell Rep.* **15**, 1945–1956 (2016).
16. T. L. Walker, R. W. Overall, S. Vogler, A. M. Sykes, S. Ruhwald, D. Lasse, M. Ichwan, K. Fabel, G. Kempermann, Lysophosphatidic acid receptor is a functional marker of adult hippocampal precursor cells. *Stem Cell Rep.* **6**, 552–565 (2016).
17. B. W. Dulken, M. T. Buckley, P. Navarro Negredo, N. Saligrama, R. Cayrol, D. S. Leeman, B. M. George, S. C. Boutet, K. Hebestreit, J. V. Pluvinage, T. Wyss-Coray, I. L. Weissman, H. Vogel, M. M. Davis, A. Brunet, Single-cell analysis reveals T cell infiltration in old neurogenic niches. *Nature* **571**, 205–210 (2019).
18. H. Stefansson, R. A. Ophoff, S. Steinberg, O. A. Andreassen, S. Cichon, D. Rujescu, T. Werge, O. P. H. Pietiläinen, O. Mors, P. B. Mortensen, E. Sigurdsson, O. Gustafsson, M. Nyegaard, A. Tuulio-Henriksson, A. Ingason, T. Hansen, J. Suvisaari, J. Lonnqvist, T. Paunio, A. D. Børglum, A. Hartmann, A. Fink-Jensen, M. Nordentoft, D. Hougaard, B. Norgaard-Pedersen, Y. Böttcher, J. Olesen, R. Breuer, H. J. Möller, I. Giegling, H. B. Rasmussen, S. Timm, M. Mattheisen, I. Bitter, J. M. Réthelyi, B. B. Magnusdottir, T. Sigmundsson, P. Olason, G. Masson, J. R. Gulcher, M. Haraldsson, R. Fossdal, T. E. Thorgeirsson, U. Thorsteinsdottir, M. Ruggeri, S. Tosato, B. Franke, E. Strengman, L. A. Kiemeney; Genetic Risk and Outcome in Psychosis (GROUP), I. Melle, S. Djurovic, L. Abramova, V. Kaleda, J. Sanjuan, R. De Frutos, E. Bramon, E. Vassos, G. Fraser, U. Ettinger, M. Picchioni, N. Walker, T. Toulopoulou, A. C. Need, D. Ge, J. Lim Yoon, K. V. Shianna, N. B. Freimer, R. M. Cantor, R. Murray, A. Kong, V. Golimbet, A. Carracedo, C. Arango, J. Costas, E. G. Jönsson, L. Terenius, I. Agartz, H. Petursson, M. M. Nöthen, M. Rietschel, P. M. Matthews, P. Muglia, L. Peltonen, D. St Clair, D. B. Goldstein, K. Stefansson, D. A. Collier, Common variants conferring risk of schizophrenia. *Nature* **460**, 744–747 (2009).
19. B. D. N. Phan, J. F. Bohlen, B. A. Davis, Z. Ye, H. Y. Chen, B. Mayfield, S. R. Sripathy, S. Cerceo Page, M. N. Campbell, H. L. Smith, D. Gallop, H. Kim, C. L. Thaxton, J. M. Simon, E. E. Burke, J. H. Shin, A. J. Kennedy, J. D. Sweatt, B. D. Philpot, A. E. Jaffe, B. J. Maher, A myelin-related transcriptomic profile is shared by Pitt-Hopkins syndrome models and human autism spectrum disorder. *Nat. Neurosci.* **23**, 375–385 (2020).
20. J. Amiel, M. Rio, L. de Pontual, R. Redon, V. Malan, N. Boddaert, P. Plouin, N. P. Carter, S. Lyonnet, A. Munnich, L. Colleaux, Mutations in TCF4, encoding a class I basic

helix-loop-helix transcription factor, are responsible for Pitt-Hopkins syndrome, a severe epileptic encephalopathy associated with autonomic dysfunction. *Am. J. Hum. Genet.* **80**, 988–993 (2007).
21. E. Kwon, W. Wang, L. H. Tsai, Validation of schizophrenia-associated genes CSMD1, C10orf26, CACNA1C and TCF4 as miR-137 targets. *Mol. Psychiatry* **18**, 11–12 (2013).
22. M. Jung, B. M. Häberle, T. Tschaikowsky, M.-T. Wittmann, E.-A. Balta, V.-C. Stadler, C. Zweier, A. Dörfler, C. J. Gloeckner, D. C. Lie, Analysis of the expression pattern of the schizophrenia-risk and intellectual disability gene TCF4 in the developing and adult brain suggests a role in development and plasticity of cortical and hippocampal neurons. *Mol. Autism.* **9**, 20 (2018).
23. M. D. Rannals, G. R. Hamersky, S. C. C. Page, M. N. Campbell, A. Briley, R. A. Gallo, B. N. Phan, T. M. Hyde, J. E. Kleinman, J. H. Shin, A. E. Jaffe, D. R. Weinberger, B. J. Maher, Psychiatric risk gene transcription factor 4 regulates intrinsic excitability of prefrontal neurons via repression of SCN10a and KCNQ1. *Neuron* **90**, 43–55 (2016).
24. H. Kim, N. C. Berens, N. E. Ochandarena, B. D. Philpot, Region and cell type distribution of TCF4 in the postnatal mouse brain. *Front. Neuroanat.* **14**, 42 (2020).
25. B. L. Kee, E and ID proteins branch out. *Nat. Rev. Immunol.* **9**, 175–184 (2009).
26. B. Cisse, M. L. Caton, M. Lehner, T. Maeda, S. Scheu, R. Locksley, D. Holmberg, C. Zweier, N. S. den Hollander, S. G. Kant, W. Holter, A. Rauch, Y. Zhuang, B. Reizis, Transcription factor E2-2 is an essential and specific regulator of plasmacytoid dendritic cell development. *Cell* **135**, 37–48 (2008).
27. H. S. Ghosh, B. Cisse, A. Bunin, K. L. Lewis, B. Reizis, Continuous expression of the transcription factor E2-2 maintains the cell fate of mature plasmacytoid dendritic cells. *Immunity* **33**, 905–916 (2010).
28. B. Fischer, K. Azim, A. Hurtado-Chong, S. Ramelli, M. Fernández, O. Raineteau, E-proteins orchestrate the progression of neural stem cell differentiation in the postnatal forebrain. *Neural Dev.* **9**, 23 (2014).
29. M. Schoof, M. Hellwig, L. Harrison, D. Holdhof, M. C. Lauffer, J. Niesen, S. Virdi, D. Indenbirken, U. Schüller, The basic helix-loop-helix transcription factor TCF4 impacts brain architecture as well as neuronal morphology and differentiation. *Eur. J. Neurosci.* **51**, 2219–2235 (2020).
30. S. Mesman, R. Bakker, M. P. Smidt, Tcf4 is required for correct brain development during embryogenesis. *Mol. Cell. Neurosci.* **106**, 103502 (2020).
31. H. Li, Y. Zhu, Y. M. Morozov, X. Chen, S. C. Page, M. D. Rannals, B. J. Maher, P. Rakic, Disruption of TCF4 regulatory networks leads to abnormal cortical development and mental disabilities. *Mol. Psychiatry* **24**, 1235–1246 (2019).
32. U. Schmidt-Edelkraut, G. Daniel, A. Hoffmann, D. Spengler, Zac1 regulates cell cycle arrest in neuronal progenitors via Tcf4. *Mol. Cell. Biol.* **34**, 1020–1030 (2014).
33. G. Berdugo-Vega, G. Arias-Gil, A. López-Fernández, B. Artegiani, J. M. Wasielewska, C.-C. Lee, M. T. Lippert, G. Kempermann, K. Takagaki, F. Calegari, Increasing neurogenesis refines hippocampal activity rejuvenating navigational learning strategies and contextual memory throughout life. *Nat. Commun.* **11**, 135 (2020).
34. S. Jessberger, R. E. Clark, N. J. Broadbent, G. D. Clemenson, A. Consiglio, D. C. Lie, L. R. Squire, F. H. Gage, Dentate gyrus–specific knockdown of adult neurogenesis impairs spatial and object recognition memory in adult rats. *Learn. Mem.* **16**, 147–154 (2009).
35. T. Goodman, S. Trouche, I. Massou, L. Verret, M. Zerwas, P. Roullet, C. Rampon, Young hippocampal neurons are critical for recent and remote spatial memory in adult mice. *Neuroscience* **171**, 769–778 (2010).
36. S.-B. Jeon, H. J. Yoon, C. Y. Chang, H. S. Koh, S.-H. Jeon, E. J. Park, Galectin-3 exerts cytokine-like regulatory actions through the JAK–STAT pathway. *J. Immunol.* **185**, 7037–7046 (2010).
37. M. Papaspyridonos, E. McNeill, J. P. De Bono, A. Smith, K. G. Burnand, K. M. Channon, D. R. Greaves, Galectin-3 is an amplifier of inflammation in atherosclerotic plaque progression through macrophage activation and monocyte chemoattraction. *Arterioscler. Thromb. Vasc. Biol.* **28**, 433–440 (2008).
38. D. Weinmann, K. Schlangen, S. André, S. Schmidt, S. M. Walzer, B. Kubista, R. Windhager, S. Toegel, H.-J. Gabius, Galectin-3 induces a pro-degradative/inflammatory gene signature in human chondrocytes, teaming up with galectin-1 in osteoarthritis pathogenesis. *Sci. Rep.* **6**, 39112 (2016).
39. X. Ma, T. Husain, H. Peng, S. Lin, O. Mironenko, N. Maun, S. Johnson, D. Tuck, N. Berliner, D. S. Krause, A. S. Perkins, Development of a murine hematopoietic progenitor complementary DNA microarray using a subtracted complementary DNA library. *Blood* **100**, 833–844 (2002).
40. X. Zhang, Y. Lan, J. Xu, F. Quan, E. Zhao, C. Deng, T. Luo, L. Xu, G. Liao, M. Yan, Y. Ping, F. Li, A. Shi, J. Bai, T. Zhao, X. Li, Y. Xiao, CellMarker: A manually curated resource of cell markers in human and mouse. *Nucleic Acids Res.* **47**, D721–D728 (2019).
41. G. Kalamakis, D. Brüne, S. Ravichandran, J. Bolz, W. Fan, F. Ziebell, T. Stiehl, F. Catalá-Martinez, J. Kupke, S. Zhao, E. Llorens-Bobadilla, K. Bauer, S. Limpert, B. Berger, U. Christen, P. Schmezer, J. P. Mallm, B. Berninger, S. Anders, A. del Sol, A. Marciniak-Czochra, A. Martin-Villalba, Quiescence modulates stem cell maintenance and regenerative capacity in the aging brain. *Cell* **176**, 1407–1419.e14 (2019).
42. N. Urbán, D. L. C. Van Den Berg, A. Forget, J. Andersen, J. A. A. Demmers, C. Hunt, O. Ayrault, F. Guillemot, Return to quiescence of mouse neural stem cells by degradation of a proactivation protein. *Science* **353**, 292–295 (2016).
43. M. A. Bonaguidi, M. A. Wheeler, J. S. Shapiro, R. P. Stadel, G. J. Sun, G. L. Ming, H. Song, In vivo clonal analysis reveals self-renewing and multipotent adult neural stem cell characteristics. *Cell* **145**, 1142–1155 (2011).
44. B. W. Dulken, D. S. Leeman, S. C. Boutet, K. Hebestreit, A. Brunet, Single-cell transcriptomic analysis defines heterogeneity and transcriptional dynamics in the adult neural stem cell lineage. *Cell Rep.* **18**, 777–790 (2017).
45. H. Hochgerner, A. Zeisel, P. Lönnerberg, S. Linnarsson, Conserved properties of dentate gyrus neurogenesis across postnatal development revealed by single-cell RNA sequencing. *Nat. Neurosci.* **21**, 290–299 (2018).
46. J. Shin, D. A. Berg, Y. Zhu, J. Y. Shin, J. Song, M. A. Bonaguidi, G. Enikolopov, D. W. Nauen, K. M. Christian, G. L. Ming, H. Song, Single-cell RNA-seq with waterfall reveals molecular cascades underlying adult neurogenesis. *Cell Stem Cell* **17**, 360–372 (2015).
47. L. Díaz-Alvarez, E. Ortega, The many roles of galectin-3, a multifaceted molecule, in innate immune responses against pathogens. *Mediators Inflamm.* **2017**, 9247574 (2017).
48. M. Gordon-Alonso, A. M. Bruger, P. van der Bruggen, Extracellular galectins as controllers of cytokines in hematological cancer. *Blood* **132**, 484–491 (2018).
49. S. Crux, J. Herms, M. M. Dorostkar, Tcf4 regulates dendritic spine density and morphology in the adult brain. *PLOS ONE* **13**, e0199359 (2018).
50. A. J. Kennedy, E. J. Rahn, B. S. Paulukaitis, K. E. Savell, H. B. Kordasiewicz, J. Wang, J. W. Lewis, J. Posey, S. K. Strange, M. C. Guzman-Karlsson, S. E. Phillips, K. Decker, S. T. Motley, E. E. Swayze, D. J. Ecker, T. P. Michael, J. J. Day, J. D. Sweatt, Tcf4 regulates synaptic plasticity, DNA methylation, and memory function. *Cell Rep.* **16**, 2666–2685 (2016).
51. M. Sepp, H. Vihma, K. Nurm, M. Urb, S. C. Page, K. Roots, A. Hark, B. J. Maher, P. Pruunsild, T. Timmusk, The intellectual disability and schizophrenia associated transcription factor TCF4 is regulated by neuronal activity and protein kinase A. *J. Neurosci.* **37**, 10516–10527 (2017).
52. N. Kyritsis, C. Kizil, S. Zocher, V. Kroehne, J. Kaslin, D. Freudenreich, A. Iltzsche, M. Brand, Acute inflammation initiates the regenerative response in the adult zebrafish brain. *Science* **338**, 1353–1356 (2012).
53. A. Ernst, K. Alkass, S. Bernard, M. Salehpour, S. Perl, J. Tisdale, G. Possnert, H. Druid, J. Frisén, Neurogenesis in the striatum of the adult human brain. *Cell* **156**, 1072–1083 (2014).
54. E. P. Moreno-Jiménez, M. Flor-García, J. Terreros-Roncal, A. Rábano, F. Cafini, N. Pallas-Bazarra, J. Ávila, M. Llorens-Martín, Adult hippocampal neurogenesis is abundant in neurologically healthy subjects and drops sharply in patients with Alzheimer's disease. *Nat. Med.* **25**, 554–560 (2019).
55. I. Bergqvist, M. Eriksson, J. Saarikettu, B. Eriksson, B. Corneliussen, T. Grundström, D. Holmberg, The basic helix-loop-helix transcription factor E2-2 is involved in T lymphocyte development. *Eur. J. Immunol.* **30**, 2857–2863 (2000).
56. T. L. Walker, G. Kempermann, One mouse, two cultures: Isolation and culture of adult neural stem cells from the two neurogenic zones of individual mice. *J. Vis. Exp.* **25**, e51225 (2014).
57. Y. Zhou, B. Zhou, L. Pache, M. Chang, A. H. Khodabakhshi, O. Tanaseichuk, C. Benner, S. K. Chanda, Metascape provides a biologist-oriented resource for the analysis of systems-level datasets. *Nat. Commun.* **10**, 1523 (2019).

Acknowledgments: We are grateful to R. Hen for providing the *NestinCre*^{ERt2} transgenic mouse line. We also thank the NCBS animal facility and Next-Generation Sequencing facility for services. **Funding:** The work was supported by funding from NCBS-TIFR, the Department of Atomic Energy, Government of India, under project no. 12-R&D-TFR-5.04-0800, and Ramanujan Fellowship (SB/S2/RJN-091/2015) from SERB-GoI to H.S.G. **Author contributions:** M.S., V.S., S.K., S.R., N (Nruthyathi), R.B., A.D., and R.C. conducted experiments and analyzed data. H.S.G. designed experiments, interpreted results, and supervised the project. B.R. provided the Tcf4-flox mouse line, and J.H. provided reagents and resources. The manuscript was written by H.S.G. with inputs from all authors. **Competing interests:** The authors declare that they have no competing interests. **Data and materials availability:** All data needed to evaluate the conclusions in the paper are present in the paper and/or the Supplementary Materials. Additional data related to this paper may be requested from the authors.

Submitted 3 November 2020
Accepted 1 April 2021
Published 21 May 2021
10.1126/sciadv.abf5606

Citation: M. Shariq, V. Sahasrabuddhe, S. Krishna, S. Radha, Nruthyathi, R. Bellampalli, A. Dwivedi, R. Cheramangalam, B. Reizis, J. Hébert, H. S. Ghosh, Adult neural stem cells have latent inflammatory potential that is kept suppressed by *Tcf4* to facilitate adult neurogenesis. *Sci. Adv.* **7**, eabf5606 (2021).